

Supporting Information

Boosting electrocatalytic nitrogen reduction to ammonia under ambient conditions by alloy engineering

Yu Jin,^{a,b} Xin Ding,^{a,b*} Linlin Zhang,^b Meiyu Cong,^b Fanfan Xu,^b Yu Wei,^a Shengjie Hao,^a Yan Gao,^{a,c*}

^a State Key Laboratory of Fine Chemicals, DUT-KTH Joint Education and Research Center on Molecular Devices, Dalian University of Technology (DUT), Dalian 116024, Liaoning, China

^b College of Chemistry and Chemical Engineering, Qingdao University, Qingdao 266071, Shandong, China

^c Ningbo Institute of Dalian University of Technology, Ningbo, 315000, P. R.China

Email: dingxin@qdu.edu.cn; dr.gao@dlut.edu.cn

Experimental Procedures

Materials

Concentrated hydrochloric acid (HCl, 37.2%), Ammonium Chloride (NH₄Cl, 99.5%), urea and Ethyl alcohol (C₂H₅OH, 99.9%) and were purchased from Chengdu Kelong Chemical Reagent Factory. Sodium hydroxide (NaOH, 99.9%), Hydrogen Peroxide Solution (H₂O₂, 30%), Hydrazine monohydrate (N₂H₄·H₂O, 50%), para-(dimethylamino) benzaldehyde (p-C₉H₁₁NO), ruthenium chloride trihydrate (RuCl₃·3H₂O), octadecene (C₁₈H₃₆, 99%) , Copper (II) chloride dihydrate (CuCl₂·2H₂O, ≥99.0%), ethylene glycol (C₂H₆O₂, AR), PVP (Polyvinylpyrrolidone, (C₆H₉NO)_n), Phloroglucinol anhydrous (C₆H₆O₃, ≥99.0%), Cyclohexane (C₆H₁₂, GC, ≥99.9%), Oleylamine (C₁₈H₃₇N, 70%) and sodium nitroferricyanide (Na₂[Fe(CN)₅(NO)]·2H₂O, 99%) were purchased from Aladdin Industrial Corp. Benzoin (C₁₄H₁₂O₂, 95%) was purchased from Sinopharm Chemical ReagentCo., Ltd. N₂ gas (99.999%), 5L of ¹⁵N₂ gas in cylinder (99%), and Ar gas (99.99%) were obtained from DALIAN NEWRADAR SPECIAL GAS CO., LTD. All the reagents were used as received without further purification. The carbon paper (CP) was purchased from Toray Industries in Japan, and was pretreated in C₂H₅OH and water for ultrasound half an hour respectively to remove the surface impurities. The deionized water used throughout all experiments was purified through a Millipore system. Nafion (DuPont, D520, 5 wt%) was diluted to 0.2% aqueous solution with mixture (C₂H₅OH: DI water = 3:1).

Synthesis of RuCu-FNs, RuCu-NPs, Ru nanomaterials, Cu nanomaterials

RuCu-FNs: In a typical preparation of RuCu-FNs, $\text{RuCl}_3 \cdot x\text{H}_2\text{O}$ (0.20 mmol), $\text{CuCl}_2 \cdot 2\text{H}_2\text{O}$ (0.10 mmol), phloroglucinol anhydrous (0.1 mmol), 12 mL oleylamine and 4 mL octadecene were added into a glass vial (volume: 30 mL). After the vial had been capped, the mixture was ultrasonicated for approximately 30 min. The resulting homogeneous mixture was then heated from room temperature to 210 °C and maintained at 210 °C for 5 h in an oil bath with argon as the protective gas. After cooling to room temperature, the resulting products were washed three times with an ethanol/cyclohexane mixture and collected by centrifugation. Catalysts with different ruthenium-copper ratios were prepared by adding 0.20 mmol $\text{RuCl}_3 \cdot x\text{H}_2\text{O}$ and 0.05 mmol $\text{CuCl}_2 \cdot 2\text{H}_2\text{O}$, 0.20 mmol $\text{RuCl}_3 \cdot x\text{H}_2\text{O}$ and 0.10 mmol $\text{CuCl}_2 \cdot 2\text{H}_2\text{O}$, 0.20 mmol $\text{RuCl}_3 \cdot x\text{H}_2\text{O}$ and 0.15 mmol $\text{CuCl}_2 \cdot 2\text{H}_2\text{O}$ and marked as $\text{Ru}_{0.80}\text{Cu}_{0.20}$ -FNs, $\text{Ru}_{0.67}\text{Cu}_{0.33}$ -FNs, $\text{Ru}_{0.57}\text{Cu}_{0.43}$ -FNs, respectively.

Ru and Cu nanomaterials: The Ru nanomaterials and Cu nanomaterials were also synthesized using the same method in the absence of $\text{CuCl}_2 \cdot 2\text{H}_2\text{O}$ and $\text{RuCl}_3 \cdot x\text{H}_2\text{O}$ respectively.

RuCu-NPs: The preparation of RuCu-NPs follows a typical process, $\text{RuCl}_3 \cdot x\text{H}_2\text{O}$ (0.20 mmol), $\text{CuCl}_2 \cdot 2\text{H}_2\text{O}$ (0.10 mmol), benzoin (0.5 mmol), 50 mg PVP were dissolved in 30 mL ethylene glycol. The mixture was ultrasonicated for approximately 30 min and then was transferred to a Teflon-lined stainless-steel autoclave and heated from room temperature to 180 °C and maintained at 180 °C for 5 h in the oven. After cooling to room temperature, the resulting products were washed three times with an ethanol/acetone mixture and collected by centrifugation.

Preparation of working electrodes

The 2 mg catalyst-nanosheets powders was dispersed in 200 μL Nafion solution thinner with ultrasonically for 1 h to produce the homogeneous catalyst ink. Then was measured 20 μL of ink and applied it evenly on pretreated carbon paper (CP, $1 \times 1 \text{ cm}^2$ Toray Industries in Japan) and dried in the air for 1 h served as a working electrode.

Characterizations

XRD data were obtained from a Shimadzu XRD-6100 diffractometer with $\text{Cu K}\alpha$ radiation (40 kV, 30 mA) of wavelength 0.154 nm (Japan). The position of the C1s peak, that is 284.4 eV, was used to correct the binding energies of all the catalysts. The high-resolution TEM (HRTEM) were carried out on microscope operated at an accelerating voltage of 200 kV. ^1H NMR spectra were obtained in D_2O -DMSO (Bruker DRX-600 NMR). The gas was measured by gas chromatography (GC 9560, Shanghai Huaai Chromatography Analysis Co., Ltd.). XPS measurements were performed on an ESCALABMK II X-ray

photoelectron spectrometer with the exciting source of Mg. UV-Vis absorption spectra were recorded on a UV-Vis spectrophotometer (Shimadzu, UV-1800). Raman spectrum was collected on Renishaw with a 532 nm laser. A gas chromatograph (SHIMADZU, GC-2014C) equipped with MolSieve 5A column and Ar carrier gas was used for H₂ quantification. Gasphase product was sampled every 1000 s using a gas-tight syringe (Hamilton). The N₂-TPD spectrum was tested by TP-5076 TPD experimental device.

Electrolyte and gas pretreatment

(1) 100 mL electrolyte was poured into the suction filter bottle, covered with a rubber stopper. Then, the gas (O₂ and N₂) in electrolyte would be removed under a vacuum pump for 30 minutes, until no bubbles were observed.

(2) The ¹⁴N₂ and ¹⁵N₂ were also purified with a gas-washing bottle filled with 3 M H₂SO₄ previously.

Electrochemical measurements

The reaction of reducing nitrogen to ammonia gas experiments were carried out in a two-channel electrolytic cell under ambient conditions, which was separated by perfluorosulfonic acid proton exchange membrane. The membrane was pretreated by first boiled in ultrapure water for 1 h and treating in H₂O₂ (5 wt%) aqueous solution at 80 °C for 1 h to remove organic impurities from carbon paper. And then, the membrane was submerged in 0.5 M H₂SO₄ for 2 h at 80 °C and finally boiled in water for 6 h. Electrochemical measurements were operated in a standard three-electrode system by a CHI660E electrochemical analyzer (CHI Instruments, Chenhua, Shanghai) using Ag/AgCl as reference electrode, and graphite rod as counter electrode and RuCu-FNs/CP (1 × 1 cm²) as working electrode respectively. Before the nitrogen reduction experiment, the HCl electrolyte (0.1 M, pH = 1) in cathode cell was bubbled with N₂ for 35 min for guaranteeing it was saturated in the electrolyte. The entire electrolytic process had sustained for two hours under each certain potential. All potentials were measured against an Ag/AgCl reference electrode and converted to the RHE reference scale using the equation: $E \text{ (vs. RHE)} = E \text{ (vs. Ag/AgCl)} + 0.197 \text{ V} + 0.0591 \times \text{pH}$ and all experiments were carried out at room temperature (25 °C).

The electrochemical activities of samples were examined by linear sweep voltammetry (LSV) with a scan rate of 5 mV/s at room temperature. Cyclic Voltammetry (CV) taken at various scan rates (10, 30, 50, 70, 90 and 110 mV/s) were recorded in the non-faradic potential range of 0.96-1.23 V vs RHE (non-faradaic region) and were used to estimate the double-layer capacitance (C_{dl}). C_{dl} was determined as the linear slope by plotting anodic current density at 1.1 V against the scan rate. $C_{dl} = i_c/v$, Where i_c represents the charging current density, v is the scan rate.

Determination of ammonia and hydrazine hydrate

The content of ammonia in the electrolyte after the reaction was measured by the indophenol blue method with some modification. 2 mL aliquot of the electrolyte was removed to color comparison tube, and add 2 mL 1 M NaOH solution containing salicylic acid (5 wt %) and sodium citrate (5 wt %), 0.2 mL of 1 wt % sodium nitroferricyanide ($\text{Na}_2[\text{Fe}(\text{NO})(\text{CN})_5]$) and 1 mL of 0.05 M NaClO, standing at room temperature for 2 h, and then measuring the UV-Vis absorption spectrum of the solution at 655nm. The hydrazine present in the electrolyte was estimated by the method of Watt and Chrisp. A mixture of para-(dimethylamino) benzaldehyde (5.99 g), HCl (concentrated, 30 mL) and ethanol (300 mL) was used as a color reagent. 5 mL aliquot of the electrolyte was added 5 mL above prepared color reagent and stirring 10 min at room temperature. The absorbance of the resulting solution was measured at 455 nm.

Calculations of NH_3 formation rate and FE

Ammonia formation rate was calculated using the following equation:

$$\text{NH}_3 \text{ yield} = 17 \times C \times V / (18 \times m_{\text{cat}} \times t)$$

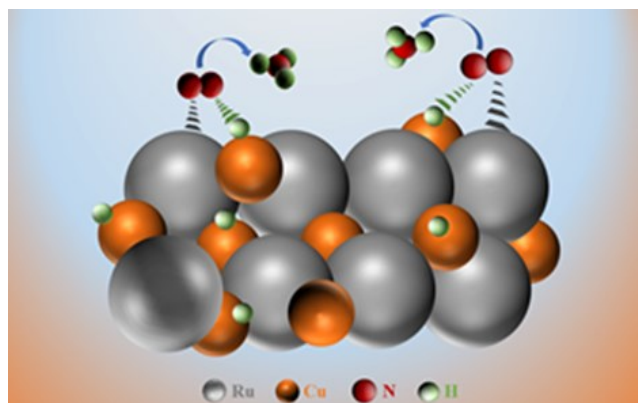
FE was calculated according to following equation:

$$\text{FE} = 3 \times C \times V \times F / (18 \times Q)$$

Where C is the measured NH_4^+ ion concentration; V is the volume of the cathodic reaction electrolyte; t is the potential applied time; m_{cat} is the loaded quality of catalyst; F is the Faraday constant; and Q is the quantity of applied electricity.

The Experiments of the ^{15}N Isotopic

The ^{15}N isotopic labeled experiment were performed using the $^{15}\text{N}_2$ isotope with the ^{15}N (99.99%) to certify the N_2 origination of ammonia. The electrolyte was pretreated to remove the dissolved N_2 and O_2 before experiment. If not, it was difficult to get $^{15}\text{N}_2$ saturated electrolyte. Then, 30 mL pretreated electrolyte was transfer to electrolytic and saturated with Ar for 30 min. Before the electrochemical reduction, the electrolyte was further saturated with $^{15}\text{N}_2$, using large flow of $^{15}\text{N}_2$ to remove the possible air above the liquid level and following small flow to get $^{15}\text{N}_2$ saturated electrolyte. After 2 h electrolysis at potential of -0.1V (vs. RHE), the resulting electrolyte was concentrated in a decompression distillation plant. The analysis of $^{15}\text{NH}_3$ product was conducted by the ^1H NMR with d^6 -DMSO.



Scheme S1 The illustration for the synergistic effect between Cu and Ru in NRR period.

Cooperative adsorption and activation was a usual pathway for NRR. Ru possessing unoccupied d orbital (Ru: $4d^7$) showed great advantage in N_2 adsorption and activation. Cooperative adsorption would happen on Ru metal in NRR process. While the cooperative adsorption also cause weak desorption, resulting in reduced performance. While, Cu with the occupied d orbital (Cu: $3d^{10}$) showed weak adsorption. In the RuCu alloy, the adjacent Cu could restrain the possible cooperative adsorption for moderate adsorption and desorption of N_2 molecule, which resulted in optimized performance. In addition, Au, Pd, Cu etc. with occupied d orbital was inclined to follow the surface hydrogenation mechanism Cu-H* would be formed firstly, and attack the N_2 molecular on adjacent Ru site. The synergistic effect between Cu and Ru caused superior performance for the lower reaction energy barrier.

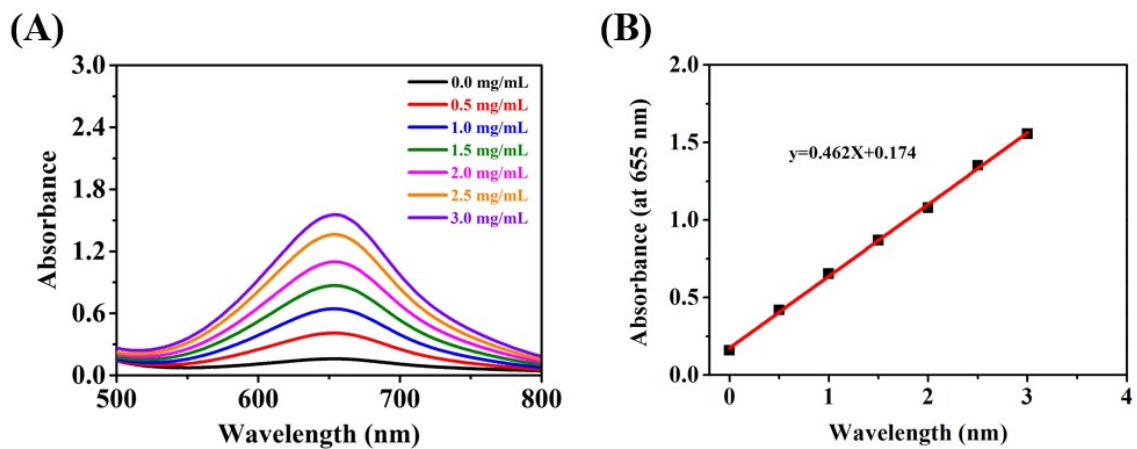


Figure S1. (A) UV-Vis absorption spectra of indophenol assays with different standard NH_4^+ concentrations after incubated for 2 h at room temperature. (B) Calibration curve used for calculation of NH_4^+ concentrations.

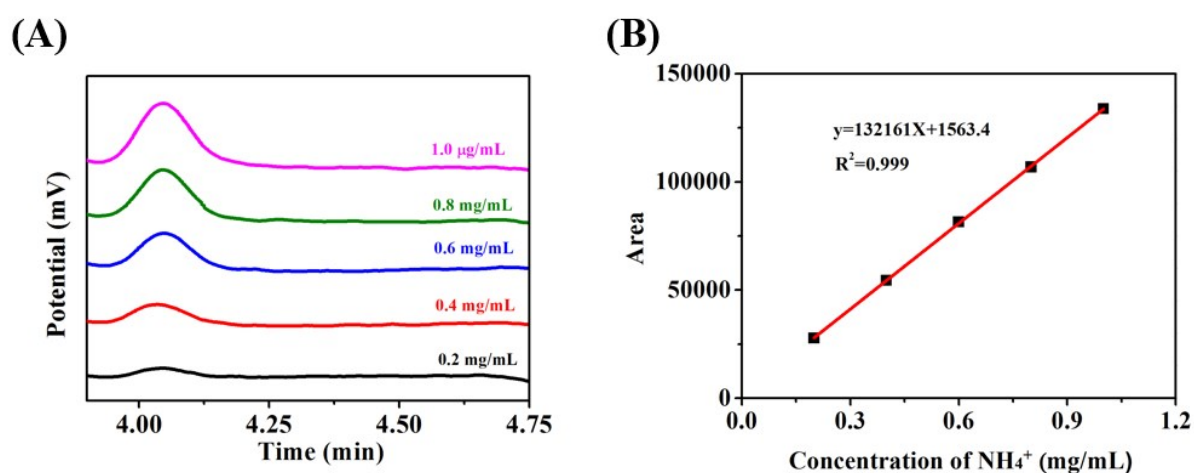


Figure S2. (A) Ion chromatogram spectra of the standard NH_4^+ concentrations (B) Calibration curve used for calculation of NH_4^+ concentrations.

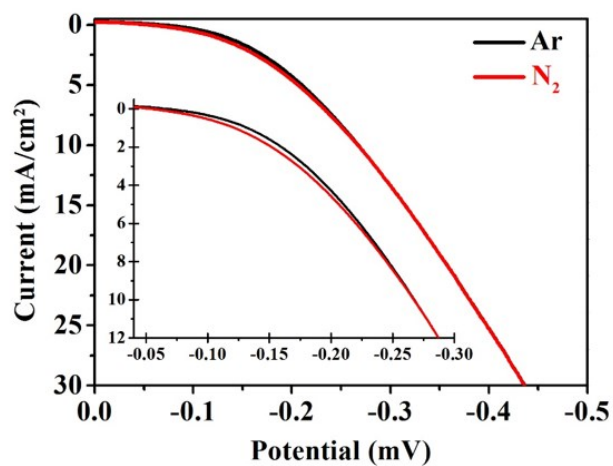


Figure S3. LSV curves for RuCu-FNs under Ar saturated and N₂ saturated electrolyte

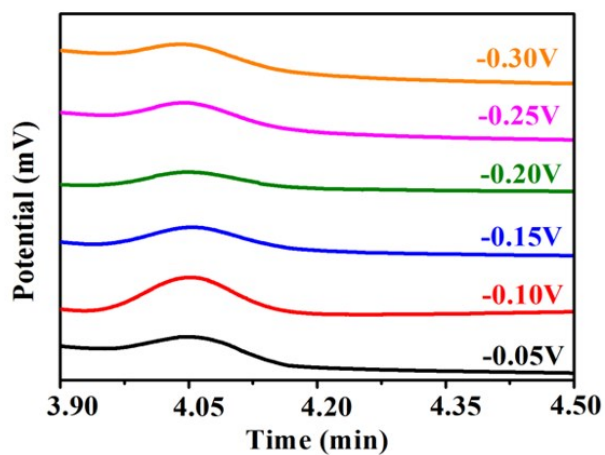


Figure S4. Ion chromatogram of the RuCu-FNs at a series of potentials after electrolysis for 2 h

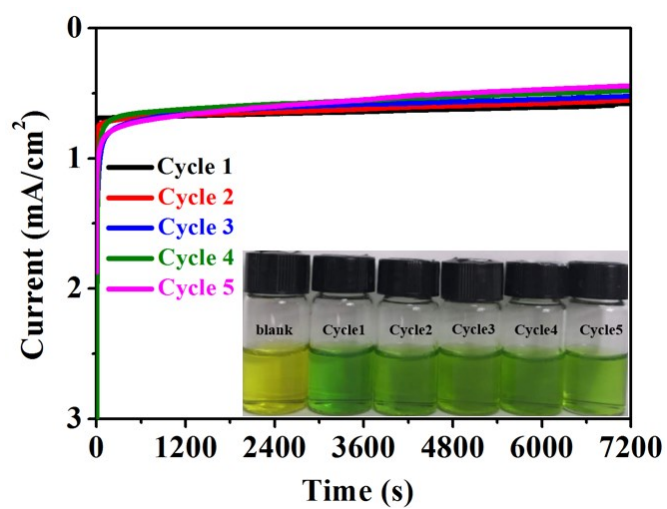


Figure S5 The current density over time during cycling tests of RuCu-FNs.

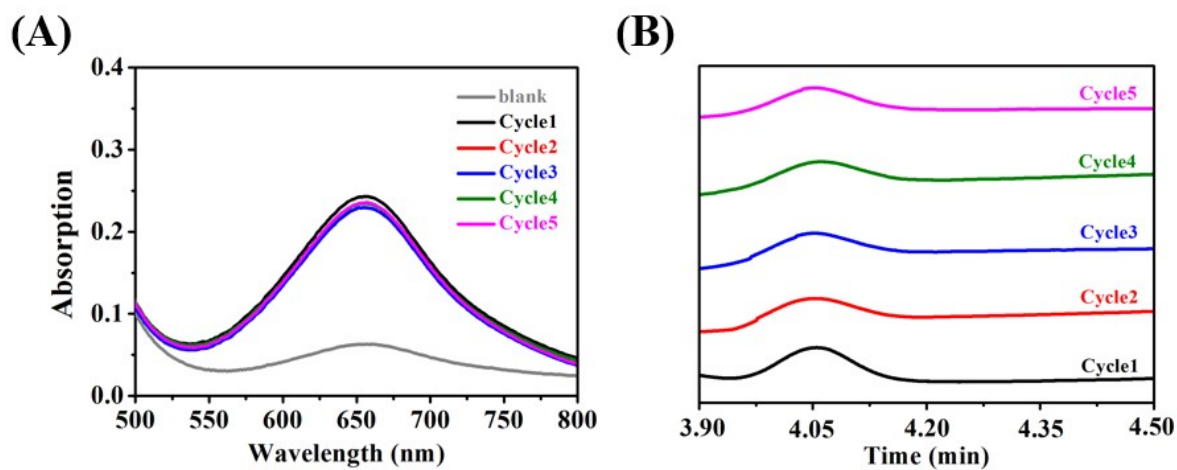


Figure S6. (A) UV-Vis absorption spectra and (B) Ion chromatogram of the RuCu-FNs at cycle tests.

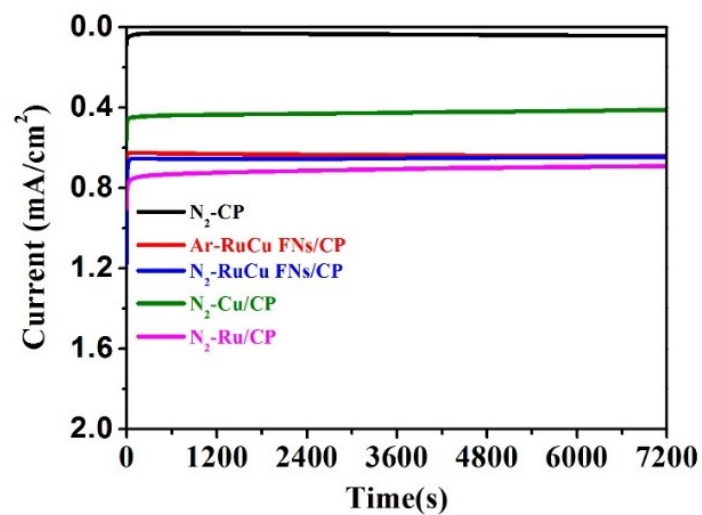


Figure S7. (A) Current density–time profiles of NRR over different catalyst at applied potential of -0.10 V vs RHE.

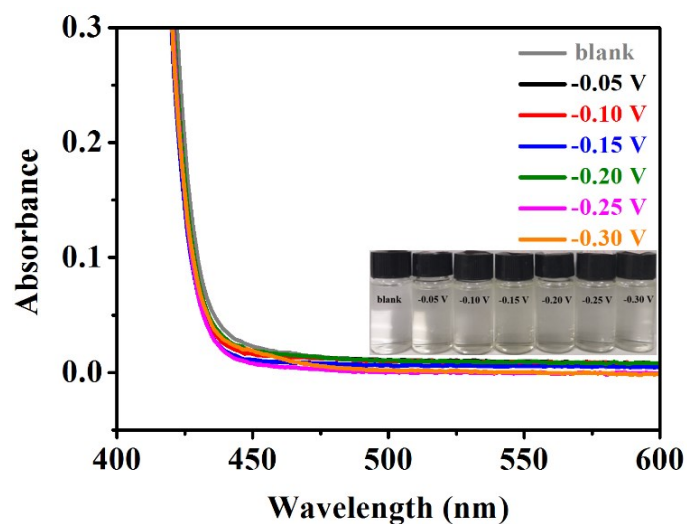


Figure S8. The yield rate of $\text{N}_2\text{H}_4 \cdot \text{H}_2\text{O}$ formation and corresponding UV-vis absorption spectra at -0.05 V to -0.30 V.

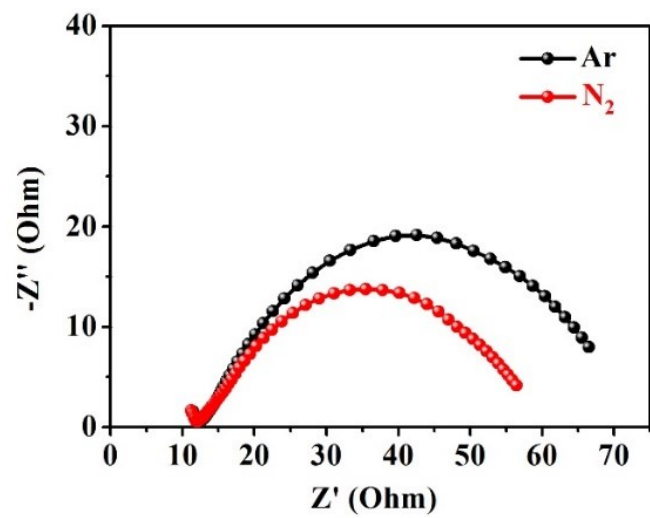


Figure S9. The electrochemical impedance measurements of the RuCu-FNs in N_2 and Ar saturated electrolytes.

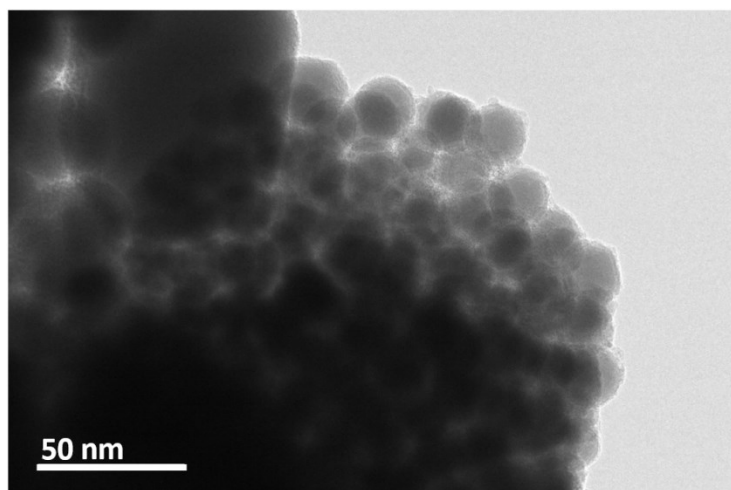


Figure S10. HRTEM images of RuCu-NPs.

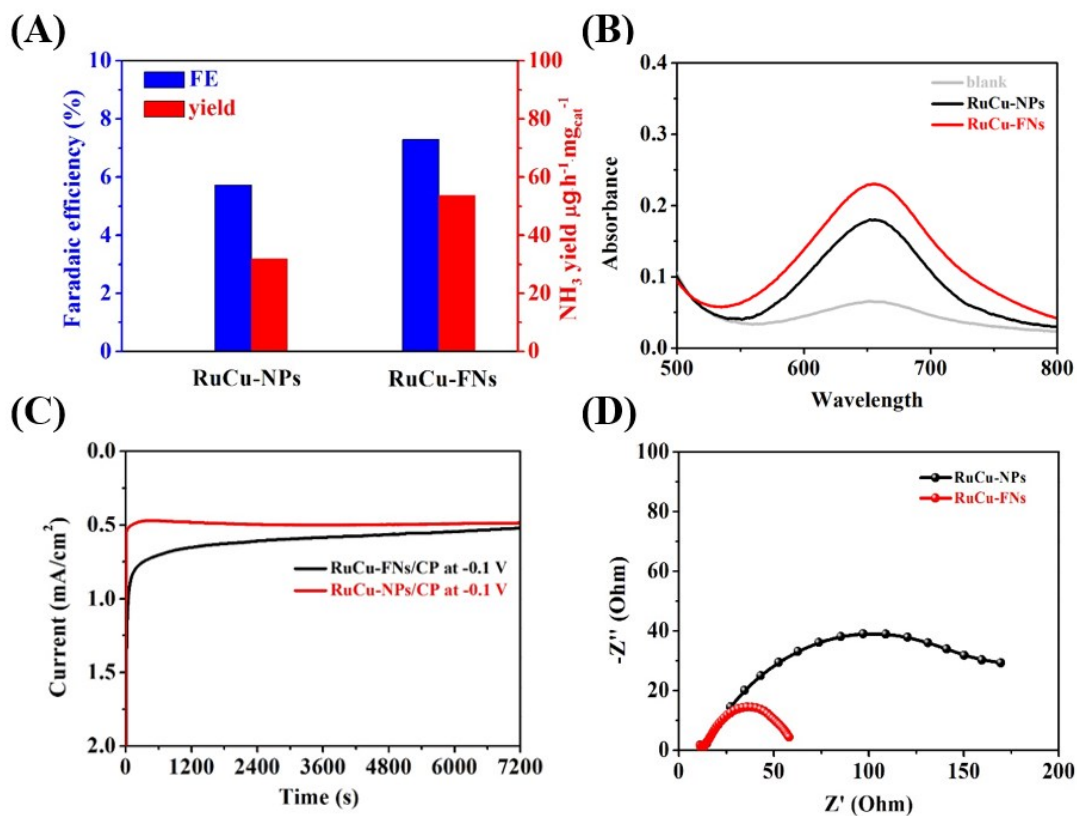


Figure S11. (A) Faradaic efficiency and NH_3 production of RuCu-NPs for NRR at -0.1V vs. RHE; (B) UV-Vis absorption spectra of the electrolytes stained with indophenol indicator in comparison experiments; (C) Chronoamperometry results of RuCu-FNs and RuCu-NPs at -0.1V vs. RHE; (D) The electrochemical impedance measurements of the RuCu-NPs and RuCu-FNs in N_2 saturated electrolytes.

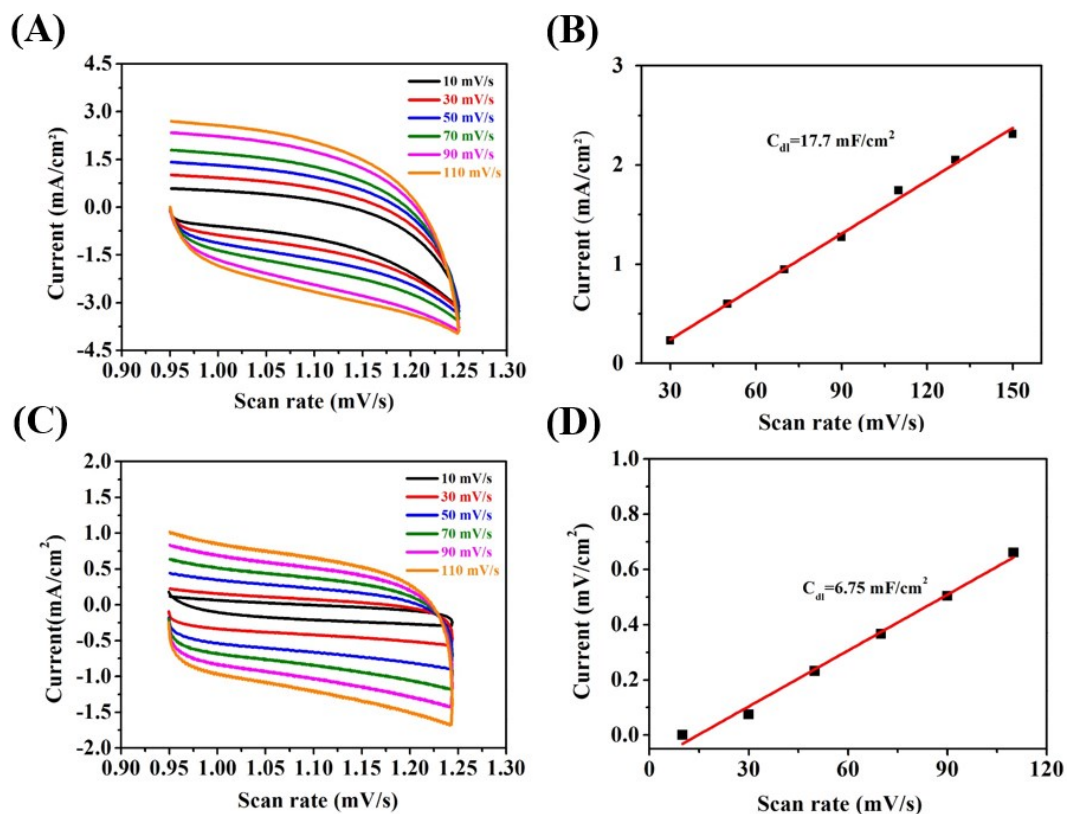


Figure S12. (A, C) Cyclic Voltammograms for synthesized RuCu-FNs and RuCu-NPs respectively at various scan rates; (B, D) charging current density of RuCu-FNs and RuCu-NPs, plotted against scan rates the double layer capacitance (C_{dl}) respectively.

RuCu nanoparticle (RuCu-NPs) was prepared for electrocatalytic nitrogen reduction. As shown in Figure S10 and 14A-C, a FE of 5.7 % and NH_3 yield rate of $32.5 \mu\text{g}\cdot\text{h}^{-1}\cdot\text{mg}_{\text{cat}}^{-1}$ was obtained for RuCu-NPs, which is lower than RuCu-FNs. The C_{dl} and the EIS results of RuCu-FNs indicate that the fusiform structure benefits enhanced performance by increasing the surface area and boosting mass transfer (Figure S11D and Figure S12).

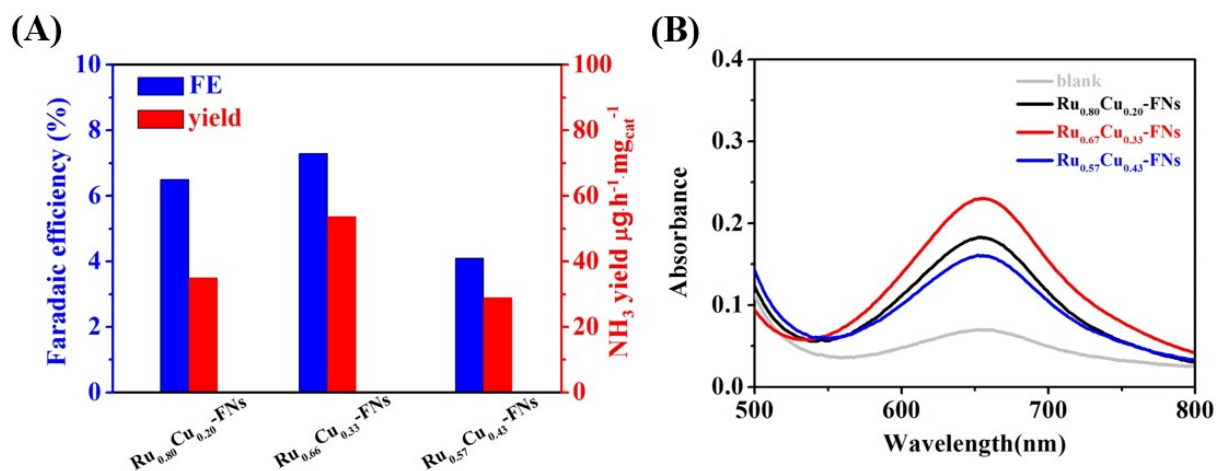


Figure S13. (A) Faradaic efficiency and NH₃ production of different ruthenium-copper ratios for NRR at -0.1V vs. RHE; (B) UV-Vis absorption spectra of the electrolytes stained with indophenol indicator in comparison experiments.

The catalysts with different ratios were also prepared and evaluated for NRR. As shown in figure S13, the Faraday efficiency and ammonia production were $35.1 \mu\text{g} \cdot \text{h}^{-1} \cdot \text{mg}_{\text{cat}}^{-1}$ (6.5%), $53.6 \mu\text{g} \cdot \text{h}^{-1} \cdot \text{mg}_{\text{cat}}^{-1}$ (7.2%), and $29.5 \mu\text{g} \cdot \text{h}^{-1} \cdot \text{mg}_{\text{cat}}^{-1}$ (4.1%), respectively. Optimal performance was obtained with a ratio of ruthenium to copper of 2:1.

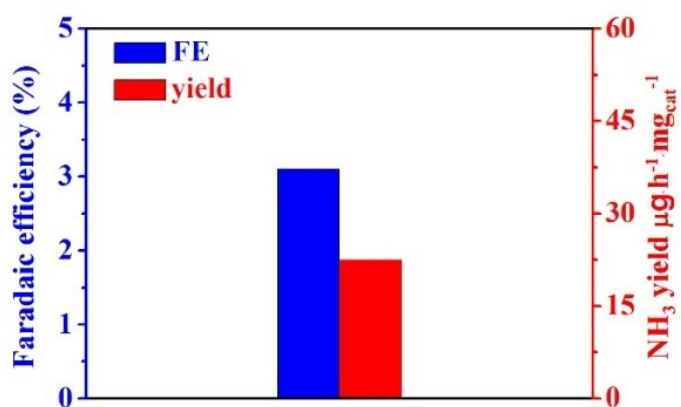


Figure S14. FE and NH₃ yields obtained for NRR of the heterogeneous mixtures of Ru and Cu at an applied potential of -0.1 V vs. RHE.

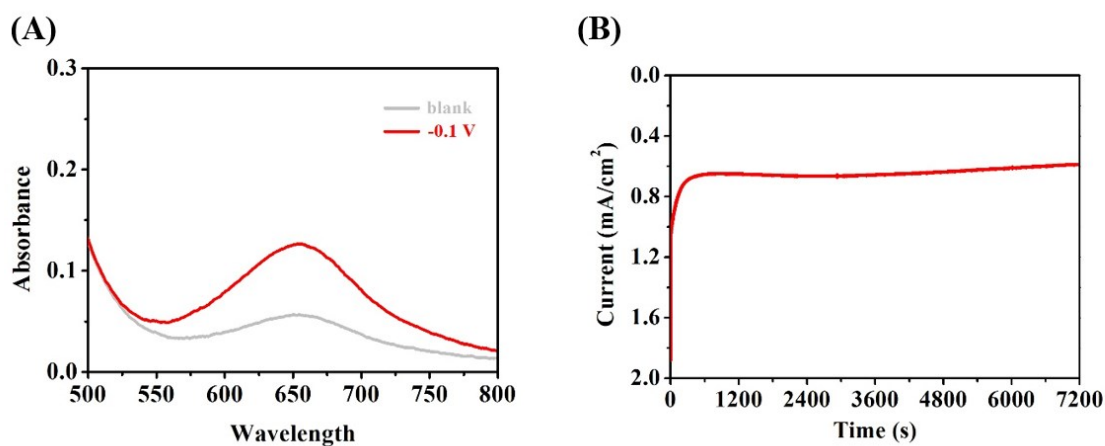


Figure S15. (A) UV-Vis absorption spectrum of the electrolytes of heterogeneous mixtures of Ru and Cu after electrolysis for 2 h at -0.1 V vs. RHE; (B) Current density–time profiles of the heterogeneous mixtures of Ru and Cu at applied potential of -0.10 V vs. RHE.

1 mg Cu and 1 mg Ru nanomaterials were dispersed in 200 μL Nafion solution thinner with ultrasonically for 1 h to obtain homogeneous catalyst ink for NRR test. As shown in Figure S14, a FE of 3.1 % and NH_3 yield rate of $22.5 \mu\text{g}\cdot\text{h}^{-1}\cdot\text{mg}_{\text{cat}}^{-1}$ was achieved, which is much lower than RuCu-FNs.



Figure S16. The resulting electrolyte was concentrated in a decompression distillation plant after electrolysis at a potential of -0.1 V (vs. RHE).